

Effect of knit and print parameters on peel strength of hybrid 3-D printed textiles

Ayushi Narula¹, Christopher M Pastore², David Schmelzeisen³, Sara El Basri³, Jan Schenk³, and Subin Shajoo⁴

Abstract

The influence of knit fabric structure on the adhesion of three-dimensional (3-D) printed textiles was examined. 3-D printing was applied to different elastic knitted fabrics with different amounts of prestretch, typical for 4-D fabric construction. The quality of the bond was measured in terms of peel strength. Peel strength was measured by pulling the fabric at 180° from the printed plastic to delaminate the 2 and recording the 10 highest peak values observed during the test. The printed width, the ratio of fabric width of print width, fabric washing, and fabric structure were varied. The specimens were then evaluated for peel strength.

Keywords

3-D printing, 4-D textiles, knit structure, porosity, peel strength

Date received: 21 September 2017; accepted: 28 December 2017

Introduction

There has been a rapid growth in research regarding three-dimensional (3-D) printing in recent years driven by the low cost and material efficiency associated with the technology. Combining 3-D printing and textile materials is still a relatively new research area.^{1–3} This represents a growth area that offers the promise of “4-D textiles”—hybrid textile/3D printed structures that can change structural form with time.

The idea of tensile structures is not new—tipis, tents, and yurts were known to the ancients. Otto was classifying and quantifying textile structures formed through tension in the early 1970s.⁴ Tensile structures depend on rigid compression elements (e.g. sticks and poles) and extensible elastic tension elements (fabrics and membranes) that combine to produce 3-D structures. What is different today is the method of producing the rigid compression elements using 3-D printing as well as the ability to design structures that can transform between two or more different configurations with nominal applied energy.

The underlying principle behind these hybrid material systems is that the stored energy in the textile material prior to printing causes a change in form when the energy is released. Typically knitted fabrics that contain elastic material, such as spandex, are used for these applications due to

the high elastic strain available and significant recovery force associated with the textile. The material chosen for these systems should be highly deformable, while maintaining enough tensile modulus to deform the printed plastic. After printing, the stored energy is released, which leads to a structural change in the system, generally changing form from a two-dimensional printed structure to a 3-D curved structure. When properly designed, it is possible to make a 3-D structure that is metastable, and thus able to assume two or more different semi-stable structural forms that can be switched back and forth with nominal energy applied.

3-D printing on textiles is used, for example, to produce jewelry,⁵ handbags, and clothing with integrated Braille.²

¹ IIT Delhi, Delhi, India

² Kanbar College of Design, Engineering and Commerce, Thomas Jefferson University, Philadelphia, PA, USA

³ RWTH Aachen University, Institut für Textiltechnik, Aachen, Germany

⁴ Karunya University, Karunya Nagar, India

Corresponding author:

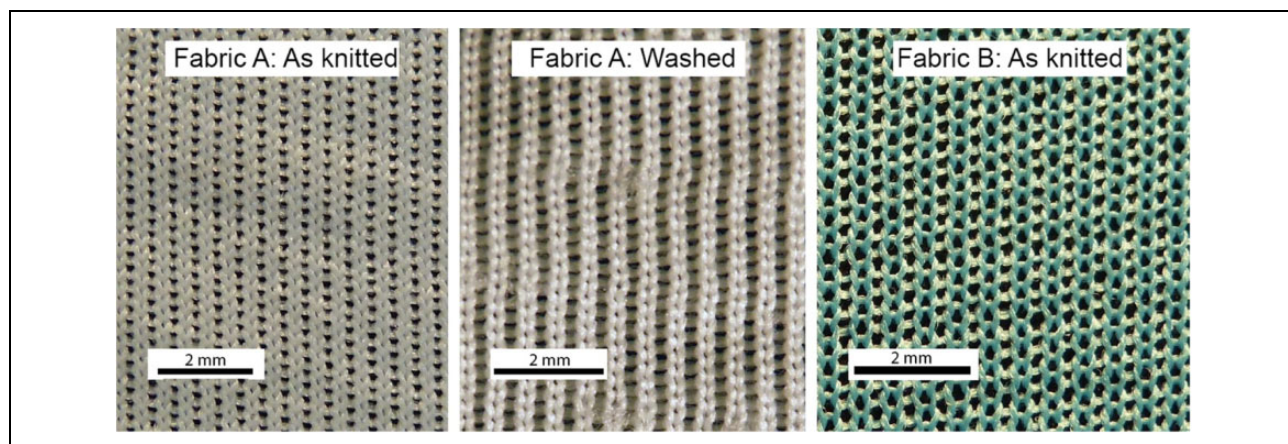
Christopher M Pastore, Thomas Jefferson University, Kanbar College of Design, Engineering and Commerce, 4201 Henry Avenue, Hayward 003-I, Philadelphia, PA 19002, USA.

Email: PastoreC@philau.edu



Table 1. Types of fabrics used in this study.

Fabric ID	Fabric style	Color	Yarn type	Yarn size (dtex)	Knitting machine gauge	Knit tension (cN)	Courses per cm	Wales per cm
A	Jersey	White	PET (PES)	70 × 2	24	6–8	20.67	24
B	Rib	Blue	PET (PES)	167	16	6	15.33	18

**Figure 1.** Photomicrographs of fabric A (as knitted (left) and washed (center)) and fabric B (as knitted (right)), all in a relaxed state. All fabrics are showing the technical face.

4-D textiles have great potential in the field of medical products, soft robotics, architecture, automotive, sports and clothing, and more. The advantages are the high customization and functional adjustment. 4-D textiles are used in size-changing objects, pressure-sensitive components,⁵ sound-absorbing textiles,⁶ and adaptive footwear.⁷

The behavior of this system depends, among other things, on the adhesion between the textile and the printed polymer. Not only does this dictate the static strength of the system but is also key to future studies around durability and reliability as the structure undergoes multiple transitions from one metastable state to another.

Typically, adhesion strength is measured through a peel test where the fabric is peeled away from the printed polymer and the force–displacement relationship is measured. There is some existing work on the adhesion strength between the fabric and the printed polymer. Studies have explored the effect of polymer temperature and print speed on the adhesion.^{2,8} In this study, we explore the effects of knit fabric structure on the peel strength of the hybrid 3-D printed textile.

Materials

Two different materials were chosen for evaluation, both weft-knitted fabrics. Fabric A is a white polyester jersey knit with intentional defects and fabric B is a blue polyester jersey knit, as shown in Table 1. Both fabrics were produced at the Institute of Technical Textiles (ITA) at RWTH Aachen University. In this preliminary study, the two fabrics were selected with different structural

parameters and knit structures rather than a parametric study based on availability.

Fabric A was considered in two states: as knitted (directly from the knitting machine) and after washing. The fabric was washed at a temperature of 30°C for 150 min at 1200 r/min. Fabric B was used as knitted only so no washed comparison is made. Images of these three fabric types are presented in Figure 1.

Prior to printing, a predetermined amount of stretch is applied to the fabrics in the warp direction. The weft (course) direction was kept at the original length, so there is a residual stress in the weft direction at the time of printing. The fabrics were marked in the relaxed state and then stretched and held in place on a plate, as illustrated in Figure 2.

The fabrics were placed with the technical back facing the print head. In the case of the jersey knit, the fabric was knitted on the front needle bed. Three different textile pre-stretch levels were used in this study—20%, 35%, and 50%. Polylactic acid (PLA) was printed onto the fabrics using a Mass Portal Pharaoh XD with a fused deposition modelling (FDM) printing mechanism for thermoplastic resins. The PLA used was a 1.75-mm diameter filament produced by Form Futura called Premium PLA. This polymer has a melt temperature of 210°C, and a melt flow rate of 0.6 g/min. The nozzle temperature during printing was 220°C and the printer bed where the fabric was located was kept at 40°C during printing. The nozzle diameter was 0.7 mm.

The polymer was printed onto the fabric in two different configurations—with a width of 10 mm and with a width of 20 mm. The choice of these dimensions was based on previous studies that showed 25 mm wide prints typically



Figure 2. Weft-knitted fabric (fabric B) stretched and held in place on a plate prior to three-dimensional printing. Pins at the edges of the plate hold the fabric still during the processing.

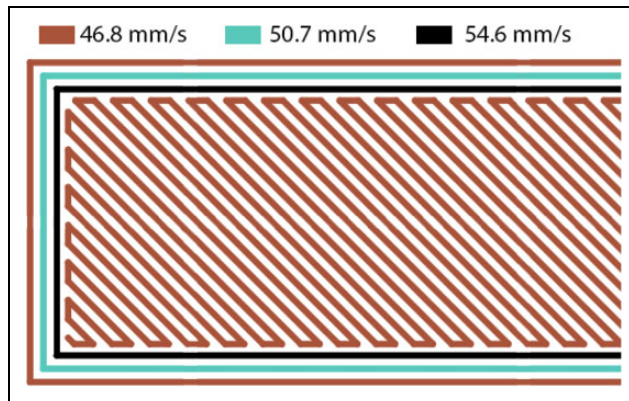


Figure 3. Schematic illustration of first layer of printing showing the rectangular edge and the diagonal fill. The different print speeds are shown in color, ranging from 48.8 mm/s to 54.6 mm/s.

resulted in tearing of the knit fabric rather than separation of the fabric from the print.

A portion of the print pattern is illustrated in Figure 3. The print used a rectangular frame followed by a diagonal infill. The print head velocity was generally 46.8 mm/s, although the inner portions of the border were printed at slightly higher velocities (50.7 and 54.6 mm/s) as shown in the figure. This figure shows only the first layer of printing. There were a total of four layers printed. Alternate layers had opposing diagonal fills in the center.

The fabric was cut after the polymer was applied, with the cut width of the fabric (compared to the width of the printed polymer) as another experimental parameter. The samples were cut so that the fabric width was 1, 2, or 3 times the width of the polymer that was printed. The length of unprinted fabric (left portion of Figure 4) was cut to be at

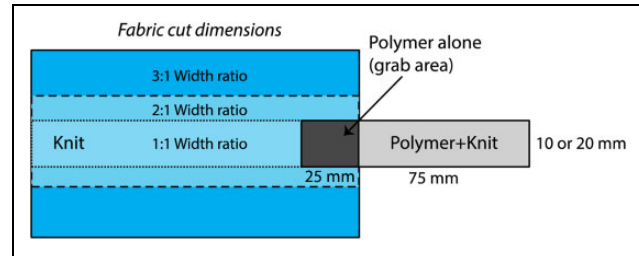


Figure 4. Schematic illustration of printing/cutting pattern for forming peel test samples.

least 100 mm. The polymer/knit area was 75 mm in length. A 25-mm long section of the printed polymer was formed without penetration into the fabric to provide a surface for grasping the polymer during testing. This was accomplished by placing a piece of tape on the fabric in this region to prevent the polymer from entering into the knit. The polymer was printed with a final thickness of 1 mm. A schematic diagram of the printing pattern is shown in Figure 4. During testing, the knit fabric is held in the lower grip (the left hand portion of the drawing) and the section marked “polymer alone” is held in the upper grip. The sample in a testing machine can be seen in Figure 12.

The first layer of printing infiltrates into the fabric and subsequent layers are above the surface of the fabric, merging with previously placed polymer and increasing the thickness of the printed material to a final thickness of 1 mm. The adhesion occurs between the textile and the first printed layer except where the tape is placed to provide a grab section for testing.

Printing was performed with a nozzle temperature of 220°C, and the print test bed was heated to 40°C prior to printing and maintained at this temperature during printing.

Figure 5 shows a photograph of an incomplete printing process on fabric B. The solid edges of the printed polymer pattern can be seen as well as the diagonal fill for the center of the printed portion.

It is anticipated that there will be both chemical and mechanical connections between the two materials, with the mechanical connection produced as a result of the polymer infiltration through the textile developed from pressure on the polymer during printing. Figure 6 shows the surface of the knitted fabric that was opposite the print head. The polymer seen in this figure has infiltrated the fabric completely.

It can be seen that the polymer infiltration produces a mushroom-shaped pillar that penetrates the fabric. Although similar, each of these is different in detailed geometry. There is an apparent randomness associated with the structure.

A range of parameters were explored in this study to evaluate their effects on peel strength addressing the effects of washing (laundering), prestretch level, sample fabric cut dimensions, and width of printed polymer, applied to two different fabric types. The parametric variation can be seen in Table 2.

Samples were produced, cut, and tested with a minimum of three replicates for each configuration. The samples

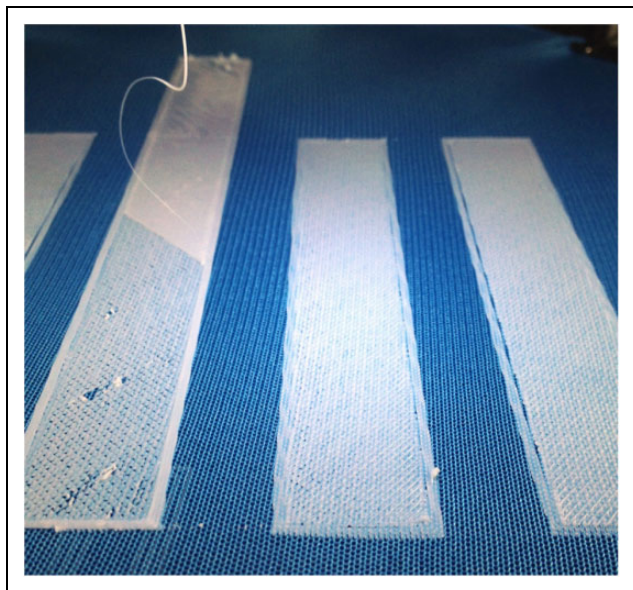


Figure 5. Fabric B during printing. The solid edges and the diagonally filled center of the printing can be seen in this photograph. The print is not complete.

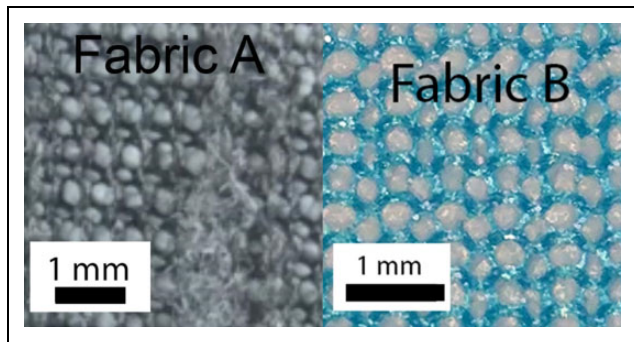


Figure 6. Fabric A (left) and fabric B (right), showing the back surface (the surface opposite the print head) after printing. The white polymer can be seen extruding through the fabric in both images. Images are not to scale with each other.

Table 2. Factors used in the experimental design.

Parameter	Variable levels
Washing	As received (O) or washed (W)
Prestretch level (%)	20, 35, or 50
Fabric to polymer width ratio	1, 2, or 3 times
Polymer width (mm)	10 or 20
Fabric type	A or B

were designated according to the factors above and this nomenclature is used in the following figures. Any sample is indicated as $A_1 N_1 - N_2 - N_3 A_2$. In this system, A_1 indicates washed (W) or as received (O), N_1 indicates the prestrain level in percent (20, 35, or 50%), N_2 indicates the fabric to polymer width ratio (1, 2, or 3), N_3 indicates the width of the polymer (10 or 20 mm), and A_2 indicates

which knitted fabric (A or B). So, for example, O20-2-10A would mean the fabric was not washed (O), had a prestrain of 20%, the fabric was twice as wide as the printed polymer, the polymer was printed at 10 mm wide, and fabric A was the textile used.

Image analysis

Photographs were made of the knit fabrics (not printed) held at different strain levels. In all cases, the course direction was kept to a fixed dimension and the wale direction was strained at levels of 0, 20, 35, and 50%. Photographs were taken of the fabric surface, and these images were processed using Adobe Photoshop® and Image-J® to collect metrics of pore geometry. In the case of the rib knits (fabric A, whether washed or not), only the large pores were considered for this analysis.

The procedure consisted of converting the image to gray scale, enhancing the contrast, and then using a threshold tool to make a binary image with the pores distinguished from the remainder of the fabric. The holes were selected and the dimensions recorded. In the case of the rib knit, the pores from the face jersey were manually removed prior to measurement. The pores were selected and processed by erosion and dilation. The selected graphical elements representing pores were reduced at the boundary by 1 pixel, expanded by 2 pixels, and finally contracted by 1 pixel. This process removes very small selections and prevents connection of regions by small artifacts. This is illustrated sequentially in the series of images in Figure 7.

After the pore selection was measured, only the selections with at least an area of 50 pixels were used for calculation purposes to avoid artifacts. The effect of prestrain on pore circularity and pore area were evaluated, and these results are shown in Figures 8 and 9. Circularity is a unitless measure, calculated as the ratio of the minor axis to the major axis of a measured object, where a value of 1 is the maximum circularity.

Not surprisingly, as the prestrain increases, the pores become less circular (more elliptical), corresponding with a single direction of strain. The longer ellipse radius corresponds with the direction in which strain is applied. Hundreds of pores were considered for each sample and the error corresponds with the variance of the individual circularity measurements.

The circularity of the pores in the jersey knit (fabric B) shows less sensitivity to strain than the rib knit. This is most likely due to the inherent fabric curvature from the complex surface of the rib knit which can extend easily at low strain levels. It appears that there is a critical transformation point for fabric B at 35% strain, but the error is sufficiently large that it is difficult to conclude if this is true or not.

The pore area (Figure 9) follows a more complex curve, suggesting there may be a local minimum that happens at some strain level, particularly to the knit structure and yarn size. It is expected that pore area should generally increase

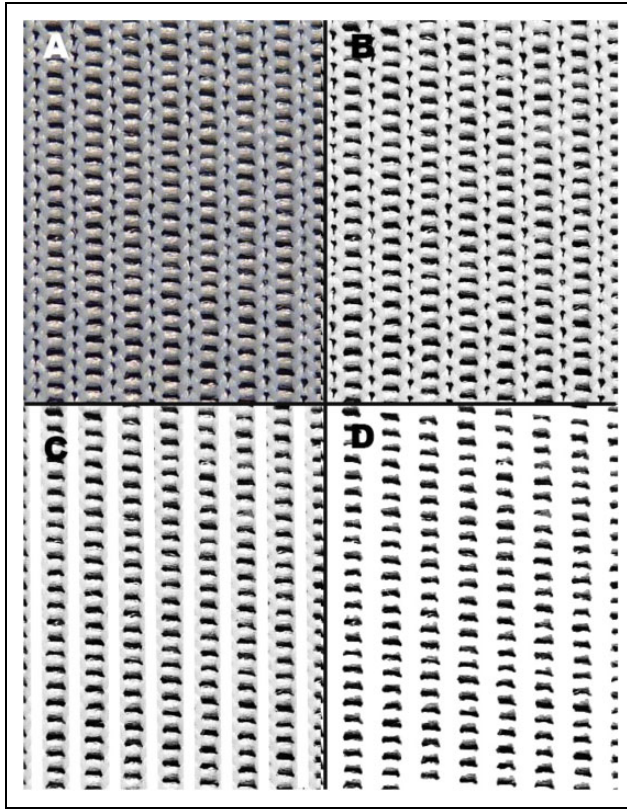


Figure 7. The various stages of image processing. Clockwise from top left, the original image (a), the grayscale image after contrast enhancement (b), the image with face jersey removed (c), and the image after binary processing and selection modification (d).

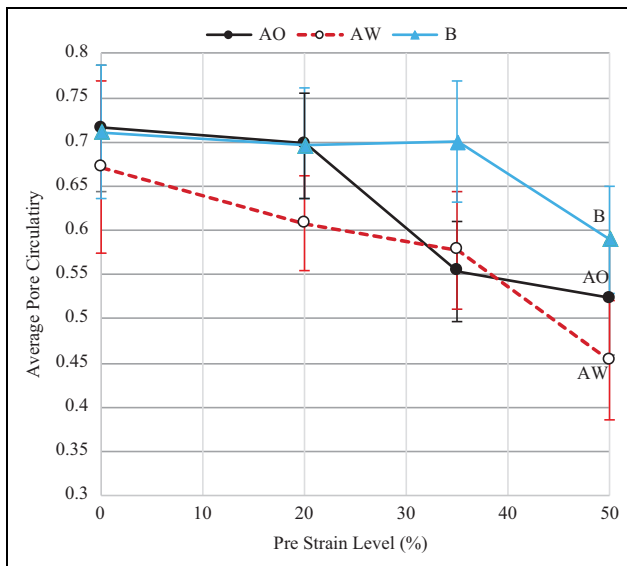


Figure 8. Effect of prestrain on the circularity of pores in the three different knitted fabric samples.

with increasing strain level, but Poisson effects, which can be quite large in knitted fabrics, may be affecting this behavior.⁹

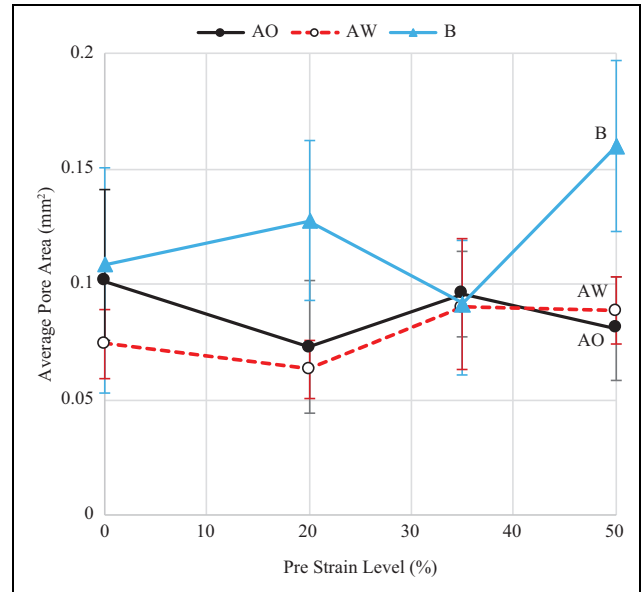


Figure 9. Effect of prestrain on the area of pores in the three different knitted fabric samples, fabric A as received (AO), fabric A after washing (AW), and fabric B (B).

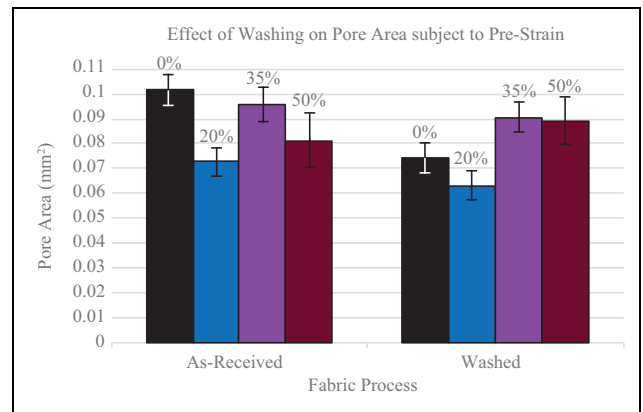


Figure 10. Comparison of average pore size of fabric A, as knitted and washed.

The pore area generally decreases after washing, except in the case of 50% prestrain, as shown in Figure 10. During washing, it is expected to see some relaxation of the knit fabric, resulting in a tighter fabric, thus smaller pores. The washed fabrics were tighter than the as-received fabrics, demonstrating a reduction texture of 13% in the course direction and 9% in the wale direction. This is also seen by the 25% reduction in pore area for the 0% prestrain AO versus AW. As the prestrain increases, the relaxation due to washing has less effect and the pore areas are closer to each other for washed and as-received.

For fabric B, in the case of 50% prestrain, there appears to be an increase in pore area, but it is not clear why this would be, or if it is an artifact of the experimental error.

The circularity of the pores (the ratio of minor axis to major axis where 1 is a circle) changed as a result of

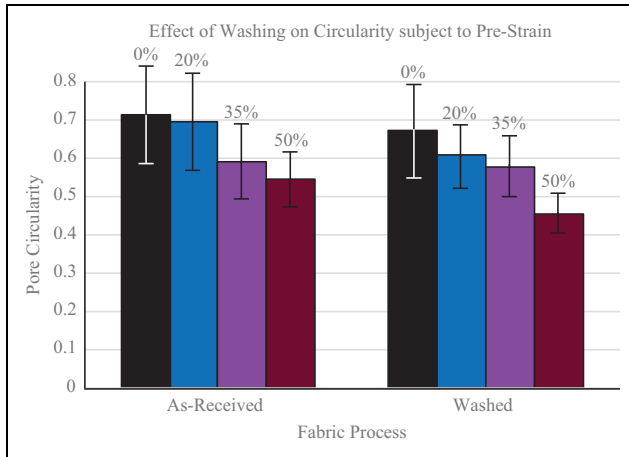


Figure 11. Comparison of pore circularity of fabric A, as-knitted and washed distinguished by prestrain levels.

washing, generally becoming less circular after washing, as shown in Figure 11. This is also attributed to relaxation of the knit fabric as a result of washing. As mentioned above, the relaxation was nonuniform, with greater relaxation in the course direction than the wale direction, resulting in less circular pores. Further, prestrain on the fabric reduces the circularity, which is expected as the strain will deform the knit structure and the pores to be more rectangular and less elliptical.

Peel testing procedure

The test procedure used in this study was developed for the materials. There are existing protocols for evaluating the bond strength between two layers of fabric (DIN 53530), but this was developed specifically for two flexible materials with an adhesive joint and was not suitable for this research. This method (DIN 53530) has been applied to the study of print adhesion to woven fabrics.¹⁰ However, the observed pull out of polymer “pins” through the knit fabrics employed in this study interfered with the results of the testing using this method.

There is a method for testing hook and loop material (ASTM D5170) and this was closer to the system at hand. A printed material with width of 10 and 20 mm was chosen to explore the effect of print width on the response of the system. Preliminary studies considered 25 mm width printing, but at this level the resistance to debonding was greater than the fabric strength and sample failed by fabric tearing rather than separation. Reducing the width to 20 mm resolved this in most cases. The samples with 10 mm width showed no difficulty with fabric tearing during testing.

Following the concept of traditional hook and loop material testing, (ASTM D5170), the material was evaluated in terms of the average of the peak loads shown in the testing. A novel test was developed for this study, involving a 180° delamination test. The fabrics were evaluated using

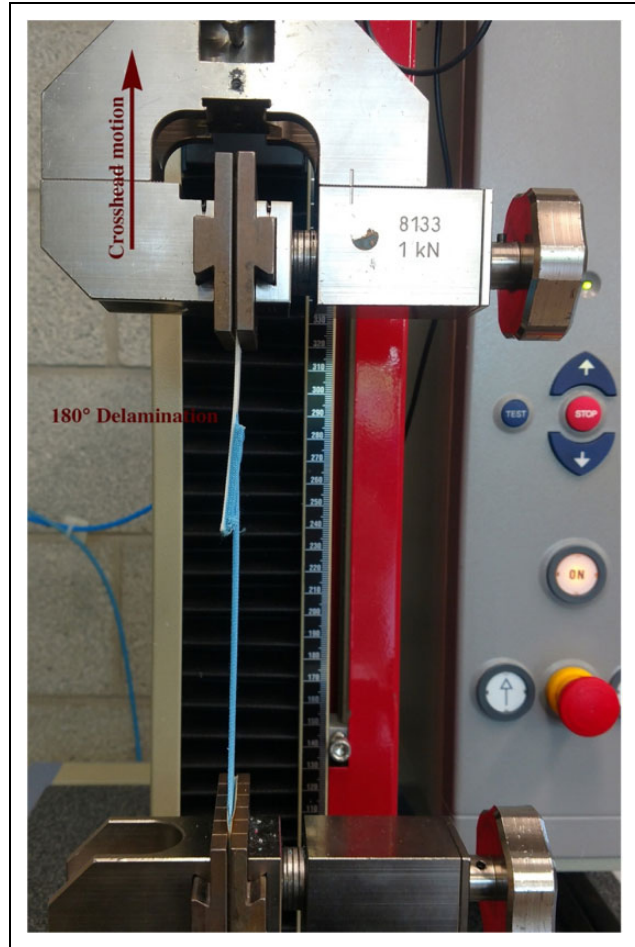


Figure 12. Photograph of Zwick tensile tester with 180° delamination sample in place.

a Zwick Z2.5 tensile tester, pulling the fabric from the printed material, as shown in Figure 12. The fabric is pulled at 180° to the printed material to create a surface of delamination, measuring force as a function of displacement.

Typical load–displacement curves showed an initial high peak, followed by lower loads. Sometimes the loads would increase as the test progressed, and in others they would decrease. There was significant variability in the results, as shown in Figure 13, a set of load–displacement curves for sample O20-3-20B (see Table 2 for description).

Significant variability was observed in all sample configurations. During the experiment, it was possible to visually observe that the peeling was nonuniform. Sometimes single pillars (see Figure 6) of polymer would pull through individually and at other times groups would pull at the same instant. The displacement is the head displacement of the tester, not directly reflecting the length of the separation between fabric and polymer. The test was stopped when the load dropped below 5 N in all cases.

The various peak loads during the test were recorded for each test and across all samples of the same configuration. The highest 10 peak loads were averaged, as illustrated

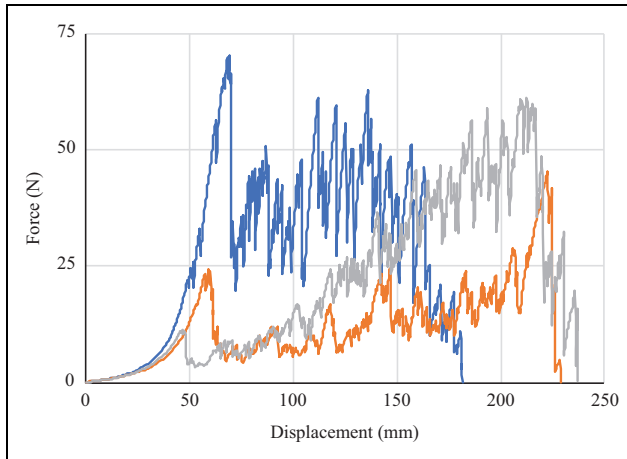


Figure 13. Typical load–displacement curves for peel tests showing the variability in performance. These three are from sample O20-3-20B, as received (not washed), 20 mm printed polymer, 3:1 fabric to polymer width ratio, 20% prestrain, fabric B.

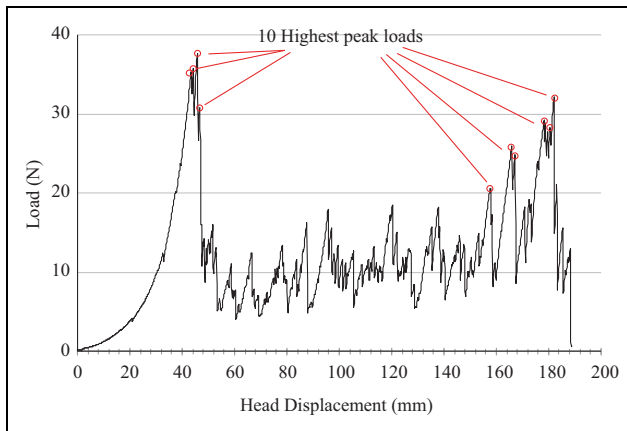


Figure 14. Illustration of highest 10 peak loads in a sample load–displacement curve. Actual calculations were performed numerically, not graphically.

in Figure 14. This value was divided by the width of the polymer to normalize, giving a value of “peel strength” for subsequent discussion.

Results

An analysis of the experimental design, using JMP (SAS), was used to analyze the test results. The input factors are listed in Table 2. The output parameters were average peak load and coefficient of variation of the average peak load. Not all possible fabric and polymer combinations were explored in this design of experiments. Figure 15 shows the effect of prestrain on the average peak load. There is no clear response behavior. Fabric A, as knitted, shows an increase in peel strength with increasing prestrain, but fabric B shows the opposite. Fabric A after washing shows a peak at 35% prestrain. Also note the size of the error bars, making a conclusive statement difficult.

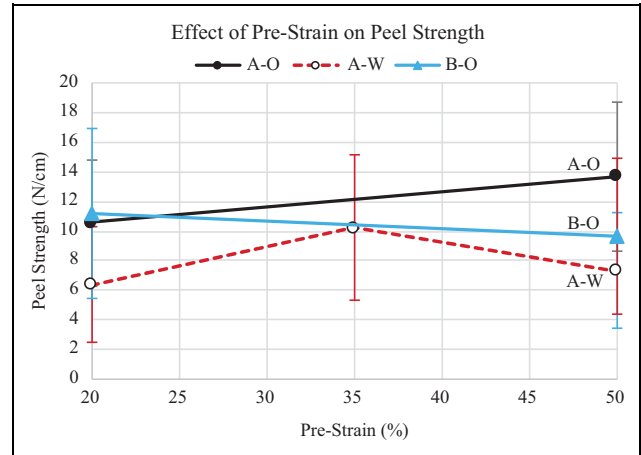


Figure 15. The effect of prestrain on the peel strength for different fabric types.

It can be seen in Figure 15 how prestrain correlates to peel strength. The sample configuration also plays a role. Figure 16 shows the effect of fabric width ratio on the reported peel strength for as-received fabrics with two different prestrain levels. It can be seen that increasing the fabric width led to increased peel strength in general, for both 10-mm- and 20-mm-wide printed polymer. This was expected from observation of the testing. Visual inspection during testing showed that fabric develops high levels of distortion near the corners where it meets the printed polymer. When the sample is wider than the printed polymer, this does not cause these large distortions at 45° to the loading direction. The greater reported values of peel strength are thought to be associated with this phenomenon.

The washed samples show a similar response to the as-received samples as shown in Figure 17. Again increasing the width of the fabric compared to the printed polymer increased the peel strength.

For some of the 1:1 samples, the fabric failed (ripped) rather than detaching from the printed polymer. It appears that increasing fabric width ratio leads to higher peel strengths, which was expected. It is recommended that at least 3:1 fabric to polymer width ratios be used in all future testing to avoid the edge effects associated with the experiment.

The width of the printed polymer also plays a role in peel strength. Figure 18 shows the effect of printed polymer width on peel strength. As the width of the polymer increases, the peel strength decreases. It is suspected that this is because the perimeter of the printed region has the highest level of adhesion because it is printed first, and subsequently the center has a lower level of adhesion. Previous investigations into print patterns¹¹ have shown that printer head speed and direction of head movement affect the infiltration of printed polymer into the knit. The printed elements in this experiment were designed with a slow print around the perimeter of the component, with the print direction aligned with the wale and course directions of the fabric. The center of the component was printed rapidly

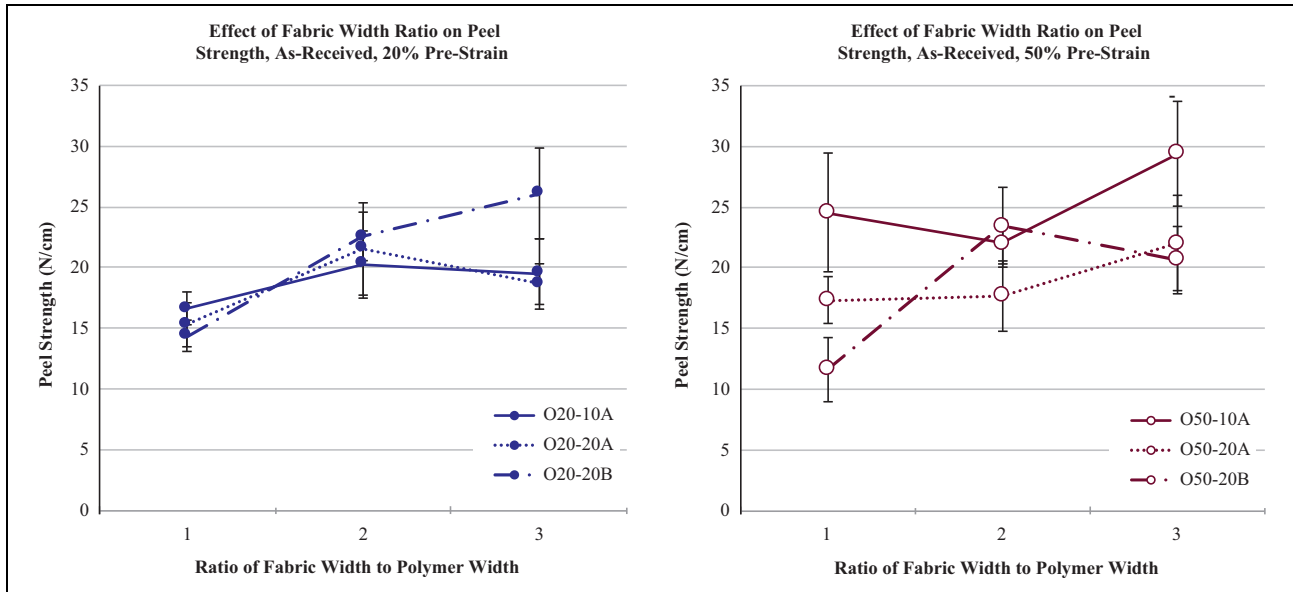


Figure 16. Effect of fabric width ratio on the peel strength, for fabrics A and B, unwashed at different prestrain levels (20% on left, 50% on right). Both 10-mm- and 20-mm-wide printed polymer were considered.

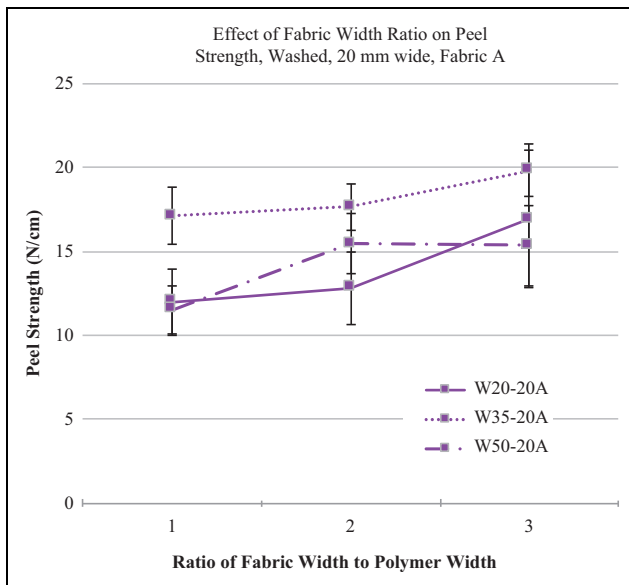


Figure 17. Effect of fabric width ratio on the peel strength, for fabric A, after washing, and with 20 mm print for different pre-strain levels (20, 35, and 50%).

using a direction running on the bias to the wale and course directions. It is presumed that the infiltration in the center is not as good as that on the perimeter. The wider component has a larger infill to perimeter ratio, and thus is expected to have a lower peel strength. This is generally confirmed by the data.

Fabric A was processed both as knitted (O) and washed (W). It was expected that washing would enhance the fiber-polymer bond, but in fact washing reduced the peel strength, as shown in Figure 19. Washing reduces the

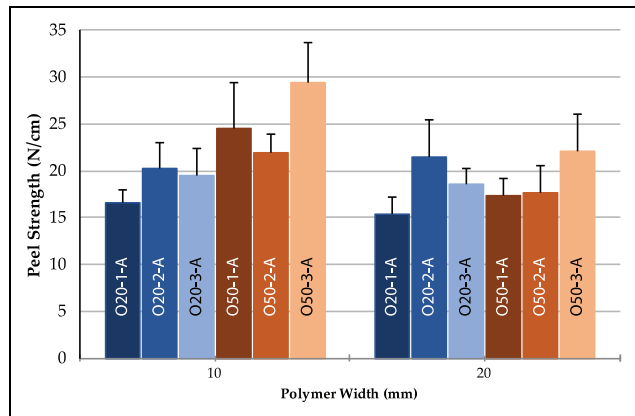


Figure 18. Effect of polymer width on peel strength. This experiment was only performed on fabric A, as knitted (O).

area of the pores through fabric relaxation, as shown in Figure 10. This reduction in pore size will also reduce the amount of infiltration of the printed polymer, which will correspondingly reduce the peel strength. It suggests that the larger scale phenomenon of resin infiltration has more impact on peel strength than the chemical interface between knitted yarn and printed polymer.

There is a dramatic loss of strength after washing. It was shown that circularity and pore size change as a function of washing, so this could be an indirect effect—not that washing reduced strength, but that washing changes pore size or circularity, which reduces strength. If we consider the correlation between pore circularity and peel strength, as shown graphically in Figure 20, there is not a clear relationship, although there is a slight relationship between increasing circularity and increasing peel strength. It is likely that a more circular pore will allow better flow of

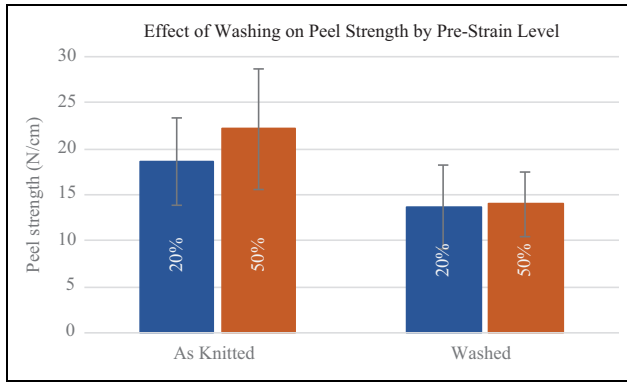


Figure 19. Comparison of peel strengths of fabric A, as knitted and washed. This graph represents the average value of samples for all width ratios and printed polymer widths.

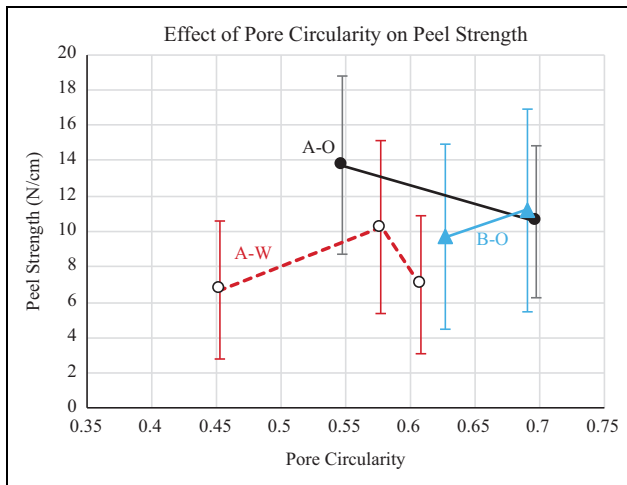


Figure 20. Relationship between pore circularity and peel strength for fabrics A and B, both as knitted (O) and after washing (W).

polymer through the pore, but it also depends on the area of the pore. The error is sufficiently large to preclude any definitive conclusion.

Looking at the correlation between pore area and peel strength also does not reveal a strong relationship, as shown in Figure 21. There is a general trend that increasing pore area increases peel strength, but it is not absolute.

If we consider peel strength to be a hook-and-loop type of interaction, it makes sense that a larger pore would have a larger “pillar” of printed polymer engaged with it, resulting in a higher peel strength. When a larger pillar is produced, not only there is more polymer infiltration into the knit structure but also the size of the “cap” of the pillar is greater, creating a stronger connection—requiring more force to remove the pillar from the knit structure. The samples in the family A-O suggest a negative relationship—higher pore areas with lower peel strengths. It is unclear why this might occur, but the experimental error is sufficiently large that this may not represent a decrease in strength.

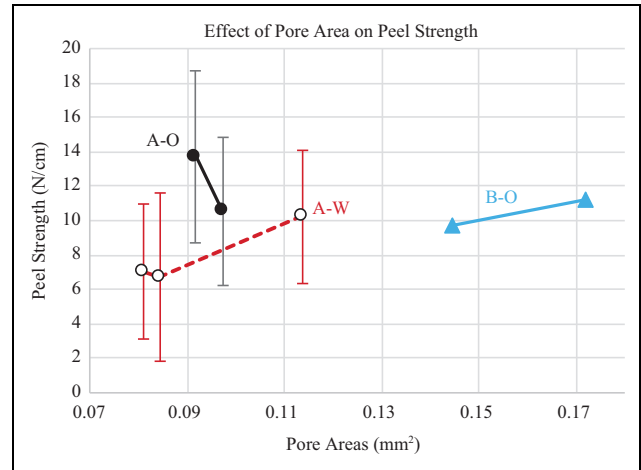


Figure 21. Relationship between pore area and peel strength for fabrics A and B, both as knitted (O) and after washing (W).

Conclusions

The energy stored in a 3-D printed prestrained textile can be used to make responsive materials, including 4-D textiles, that will find applications in a broad range of industrial sectors. The need exists to make these structures rugged and durable. To that end, it is necessary to understand the interface between textile and printed polymer.

In this study, we explored several factors such as print area ratios, prestretch, and fabric characteristics (fabric structure, fabric density, and pore geometry) to determine their effects on polymer–textile adhesion.

A decrease in pore area and circularity after washing is observed, which suggests the need of the pretreatments to be customized so as the shrinkage in the textile is reduced, or that the postwashed parameters are used for design purposes. Combining these factors, an indirect relationship between pore structure and peel strength can be observed. More circularity generally gives better peel strength.

The specific test configuration plays a significant role in the performance of the samples. Test standards DIN 53530 and ASTM D5170, designed for similar yet different evaluations, may not be the best choice for evaluating these materials. When the printed sample is too wide (25 mm), the test resulted in fabric tearing with little separation of the two materials. Changing the sample print width to 10 and 20 mm allowed the experiment to show separation. As the polymer width decreased, the peel strength (force per unit width) increased. This change in width is also associated with the print pattern which has a different border than interior.

The relative width of the fabric compared to the printed polymer was also shown to have an effect on the performance of the sample. As the fabric width exceeded the printed polymer width, the peel strength generally increased. Visual observation suggests that the thinner fabric has stress concentrations at the corners of the printed material, and these were reduced with wider fabric samples. It is suggested

that tests of these types be performed with fabrics 2 to 3 times as wide as the printed polymer.

Overall, the results suggest that the adhesion between polymer and textile is controlled more significantly by mechanical effects than chemical. With the correct set of parameters, the adhesion can be improved substantially to open the doorways to new programmable and responsive 4-D textiles.

Declaration of conflicting interests

The author(s) declared no potential conflicts of interest with respect to the research, authorship, and/or publication of this article.

Funding

The author(s) received no financial support for the research, authorship, and/or publication of this article.

ORCID iD

Christopher M Pastore  <http://orcid.org/0000-0003-4272-3808>

References

1. Brinks GJ, Warmöskerken MMC, Akkerman R, et al. *The added value of 3D polymer deposition on textiles*. Dresden, 2013.
2. Pei E, Shen J and Watling J. Direct 3D printing of polymers onto textiles: experimental studies and applications. *Rapid Prototyp J* 2015; 21: 556–571.
3. Sabantina L, Kinzel F, Ehrmann A, et al. Combining 3D printed forms with textile structures – mechanical and geometrical properties of multi-material systems. *IOP Conf Ser Mater Sci Eng* 2015; 87: 1–5.
4. Otto F, Trostel R and Schleyer FK. *Tensile structures; design, structure, and calculation of buildings of cables, nets, and membranes*. Cambridge, Mass: The MIT Press, 1973.
5. Rivera ML, Moukperian M, Ashbrook D, et al. Stretching the bounds of 3D printing with embedded textiles. In: Mark G, Fussell S, Lampe C, et al. (eds) *Proceedings of the 2017 CHI conference on human factors in computing systems - CHI '17*, New York, USA: ACM Press, 2017, pp. 497–508.
6. Clasen D, Wallasch M, Köneke O, et al. *Sonogrid*, <http://sonogrid.de/konzept/> (2017, accessed 27 April 2017).
7. Guberan C, Clopath C and Tibbits S. *Active Shoes*, <http://www.selfassemblylab.net/ActiveShoes.php> (accessed 14 May 2017).
8. Sanatgar HR, Campagne C and Nierstrasz V. Investigation of the adhesion properties of direct 3D printing of polymers and nanocomposites on textiles: effect of FDM printing process parameters. *Appl Surf Sci* 2017; 403: 551–563.
9. Abou-Iiana M, Youssef S, Pastore C, et al. Assessing structural changes in knits during processing. *Text Res J* 2003; 73: 535–540.
10. Korgor M, Bergschneider J, Lutz M, et al. Possible applications of 3D printing technology on textile substrates. *IOP Conf Ser Mater Sci Eng* 2016; 141: 01 2011.
11. Ayranci C. Additive manufacturing of shape memory polymers, part 1: effects of print orientation and infill percentage on mechanical properties. *Rapid Protot J* in press; 24.